https://doi.org/10.15407/ufm.27.02.221

V.V. KYRYLCHUK [1,*], V.K. NOSENKO [1,], B.S. BAITALYUK [1], I.K. YEVLASH [1], A.V. NOSENKO [1,***], V.E. IAKOVLEV [1], M.S. NIZAMEYEV [1], and V.A. DEKHTYARENKO [1,2,****]**

[1] G.V. Kurdyumov Institute for Metal Physics of the N.A.S. of Ukraine, 36 Academician Vernadsky Blvd., UA-03142 Kyiv, Ukraine

[2] E.O. Paton Electric Welding Institute of the N.A.S. of Ukraine, 11 Kazymyr Malevych Str., UA-03150 Kyiv, Ukraine

* kyrylchuk_v@ukr.net, ** victorn58@ukr.net, *** itrij@ukr.net, **** devova@i.ua

AMORPHOUS ALLOYS AS A PROMISING CLASS OF FUNCTIONAL MATERIALS. Pt. 2. Magnetic Properties, Magnetic Anisotropy, and Disaccommodation

This work is concerned with a well-known class of functional materials, namely, ribbon amorphous metal alloys based on Fe and Co. Their magnetic properties are analysed, in particular, the features of the formation of magnetic anisotropy, the phenomena of magnetic after-effects (disaccommodation), as well as the influence of thermal and thermomagnetic treatments on them. The physical nature of their magnetic softness, the role of local and macroscopic magnetic anisotropy, magnetoelastic effects, magnetostriction, and domain structure in the formation of the magnetisation reversal loop are revealed. The main sources of their magnetic anisotropy are indicated, among which the magnetoelastic anisotropy due to internal stresses and magnetostriction, as well as the anisotropy of directional ordering of atomic pairs, play a decisive role. In addition, the given magnetic anisotropy is a thermally activated process, the driving force of which is the interatomic magnetic interaction, and the efficiency of its formation increases with a decrease in the magnetostriction of the alloy. The mechanisms of induction of uniaxial anisotropy during annealing in a magnetic field and thermomechanical processing are presented, as well as their influence on the coercive force, magnetic permeability, and magnetisation reversal losses. As determined, the temperature

Citation: V.V. Kyrylchuk, V.K. Nosenko, B.S. Baitalyuk, I.K. Yevlash, A.V. Nosenko, V.E. Iakovlev, M.S. Nizameyev, and V.A. Dekhtyarenko, Amorphous Alloys as a Promising Class of Functional Materials. Pt. 2. Magnetic Properties, Magnetic Anisotropy, and Disaccommodation, *Progress in Physics of Metals*, **27**, No. 2: 221–251 (2026)

and time instabilities of their magnetic properties are associated with the stabilisation of domain boundaries due to directional atomic ordering, and their study is carried out using disaccommodation. The prospects of using amorphous soft magnetic materials with zero magnetostriction in modern mid-range- and high-frequency electromagnetic devices are shown.

Keywords: amorphous metal ribbon, magnetic properties, thermal and thermomagnetic treatments, magnetic anisotropy, disaccommodation.

1. Introduction

According to the data presented in the works [1, 2], for the first time, amorphous alloys by steam quenching and electrodeposition were obtained back in the 50s of the last century. The beginning of the development of amorphous metal alloys is considered to be the years 1959–1960, when a method of obtaining an amorphous structure by direct cooling of the melt was invented [3, 4]. As the authors note [2], the first samples with an amorphous structure were obtained in small quantities, since pistons were used to cool the melt, which flattened the drops and cooled them at a very high speed [4]. The invention of a method for obtaining an amorphous ribbon of great length gave a significant impetus to the research of amorphous materials.

Amorphous metal alloys are characterized by the absence of long-range order in the arrangement of atoms (translational symmetry). That is why they do not have such defects of atomic structure specific to crystalline bodies as [5, 6]: dislocations and vacancies; grain and block boundaries; twins and packing defects. The amorphous state is characterized not only by close to ideal atomic-structural homogeneity, due to the absence of the defects listed above, but also by high phase–chemical homogeneity. Essentially amorphous materials, regardless of the nature and concentration of the components, represent a single-phase system — a supersaturated solid solution, the atomic structure of which is similar to the atomic structure of a supercooled melt [7, 8]. These features of the structure of amorphous alloys determine not only the complex of physical and mechanical properties characteristic of them, but also their unique combination [1].

According to the data presented in the works [9, 10], the formation of an amorphous structure can be facilitated by: a significant (not less than 15%) difference in the atomic radii of the components (for example, transition metals and metalloids); a large difference in the valence of the materials used; the presence in the alloy of more than three components, which are characterized by large negative enthalpies of mixing (ΔH^{mix}).

Amorphous alloys are characterized by extremely low losses on magnetization reversal, which determines their wide application in radio electronics and instrument making [11–13]. The amorphous phase obtained as a result of ultrafast cooling of the melt is metastable in relation to the

crystalline state, and its atomic structure immediately after obtaining is non-equilibrium [14]. The amorphous phase can be brought into a state of relative equilibrium by annealing carried out below the crystallization temperature [15–17]. The processes, which occur during the heat treatment of the amorphous phase and bring it into a state of metastable equilibrium, are defined as structural relaxation processes [1]. The course of relaxation processes is accompanied by a change in all physical and mechanical properties of amorphous alloys. By varying the heat treatment conditions, it is possible to change the physical properties of amorphous alloys in the desired direction. In general, structural relaxation is considered one of the most fundamental phenomena inherent in amorphous alloys. A characteristic feature of structural relaxation in amorphous alloys is that some of the relaxation processes are irreversible, while others are reversible [1]. Accordingly, some physical properties of amorphous alloys are also irreversible, while others exhibit the effect of reversibility.

In addition to the above advantages, amorphous alloys also have certain disadvantages, which somewhat restrain their widespread use in modern technology [18–22]. The main ones are as follow: a tendency to embrittlement; temperature–time instability; significant dependence of magnetic properties on the conditions of amorphization and heat treatment. As a result of heat treatment, amorphous alloys can change their magnetic properties to a wide extent, both in the direction of their improvement and deterioration. That is why the establishment and physical justification of heat treatment modes, including those carried out in magnetic fields, which ensure their maximum achievable optimal level, remains an urgent task today.

2. Magnetic Properties. Effect of Thermal and Thermomagnetic Treatments

It is known that in ferromagnetic materials each magnetic atom has a significant magnetic moment, which is associated with quantum-mechanical exchange interaction with neighbouring moments [23].

Below the Curie temperature, T_C, the exchange energy becomes sufficient to overcome thermal disorder, which leads to spontaneous magnetisation. The total magnetisation $\vec{M}$ is just the vector sum of the moments of all individual atoms. Accordingly, the induction is $\vec{B} = \mu_0\vec{H} + \vec{M}$.

In a soft magnetic alloy (particularly, in amorphous metal alloys based on Fe and Co), $\vec{M}$ easily follows the external magnetic field (H), because of which the relative magnetic permeability $\mu = \dfrac{\vec{B}}{\mu_0\vec{H}}$ can reach $>10^5$ [24–27]. Figure 1 shows a unique combination of saturation induction B_s and effective magnetic permeability m_e at a frequency of 1 kHz for typical soft magnetic iron-based alloys [28].

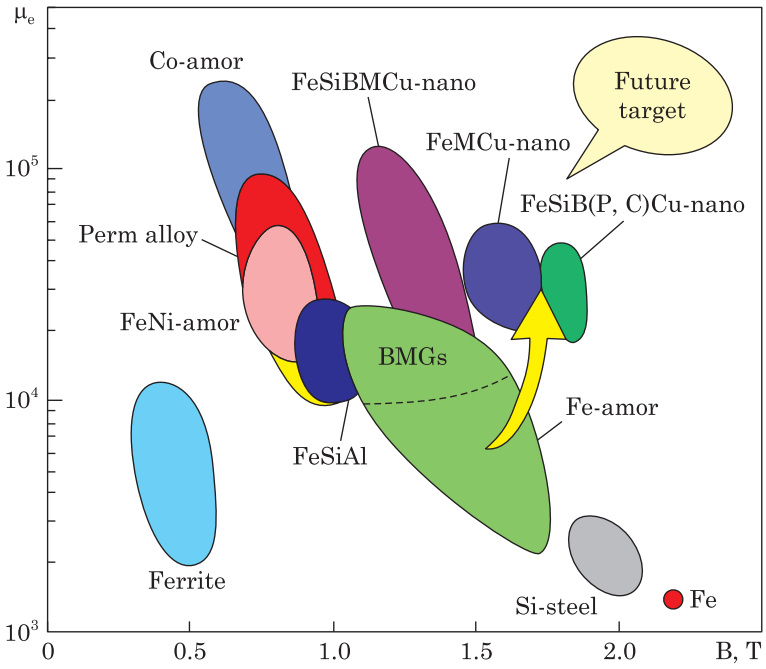

Fig. 1. Saturation magnetic induction and effective permeability (1 kHz) of typical soft magnetic alloy materials [28]

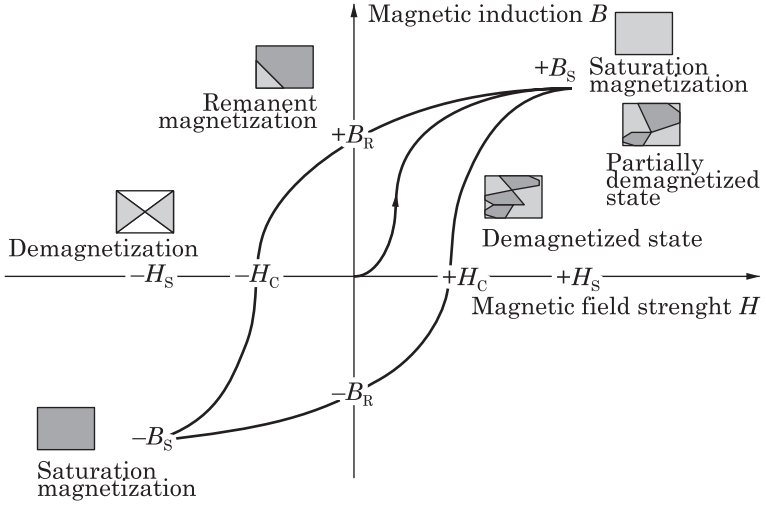

Fig. 2. Hysteresis loop [24]

In magnetic materials, there is hysteresis (Fig. 2), that is, between the induction (B) and the magnetic field ($\vec{H}$), there is a nonlinear non-local relationship, which is parametrically displayed in the form of a loop [24].

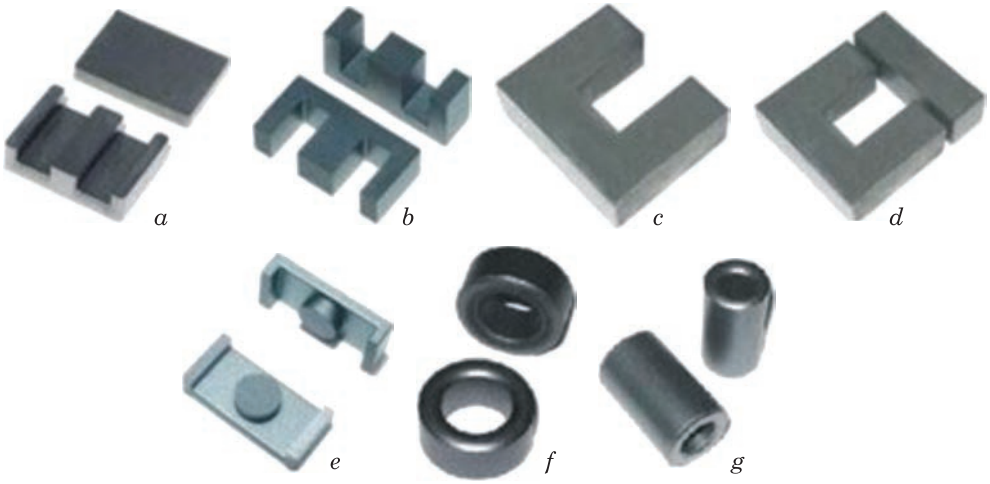

Fig. 3. Different shapes of ferrite cores: (*a*) E–I core, (*b*) E–E core, (*c*) U core, (*d*) U–I core, (*e*) EER core, (*f*) toroidal core, and (*g*) tube core [36]

According to the magnitude of the coercive force, H_c, soft magnetic (<100 Oe) and hard magnetic (>100 Oe) materials are distinguished [29].

For a ring core with a centreline length l_m and a cross-sectional area A_c, the current $i(t)$ flowing in a winding with the number of turns N creates an external field $H(t) = Ni(t)/l_m$. According to Faraday's law, the voltage at the terminals of the winding is equal to [30, 31]

$$V(t) = i(t)R_w - NA_c \frac{dB(t)}{dt}, \tag{1}$$

where R_w is the ohmic resistance of the winding.

In the case of using a thick wire to form the winding, the side losses, i^2R_w, can be neglected. Then, the energy losses in the inductor (or transformer) P_L, which are dissipated during the period of the excitation current $i(t)$, are described by the equation [32]

$$P_L = \int_{t=0}^{T} i(t)V(t)dt = l_m A_c \int H(t)dt \frac{dB}{dt} = l_m A_c \oint HdB = P_l. \tag{2}$$

It is obvious that the losses per period per unit volume of the core are determined by the area of the dynamic hysteresis loop. The inductance of the coil L and, accordingly, P_L depend on the hysteresis properties of the material and the shape of the core. That is why the development programs of soft magnetic materials, including amorphous alloys, are aimed at implementing hysteresis loops of various types with the required properties. This can be achieved by choosing the chemical composition of the alloy, thermal or thermomagnetic treatment, thermomechanical processes and core geometry (core shape: *I*, *U*, *O* — type with and without non-magnetic gaps) [33–35] (Fig. 3).

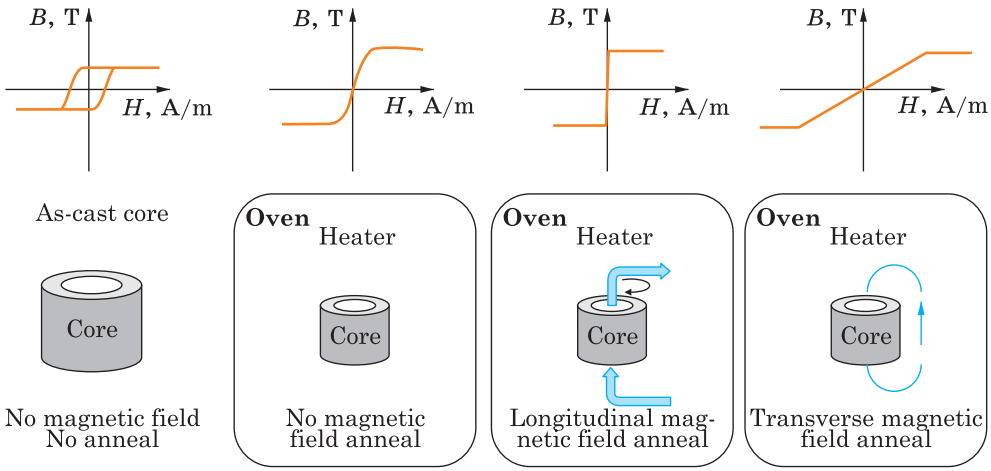

Fig. 4. Hysteresis loops versus various heat treatments of soft ribbon magnetic ring [12]

There are several types of hysteresis loops of amorphous alloys, which are created by the above method (Fig. 4).

(1) Round (flat) loop (K_n = 0.3–0.6), characterized by a high initial magnetic permeability $\mu_i \approx$ 30–100 thousand (achieved by selecting the composition and simple heat treatment above the T_C with subsequent rapid cooling). Annealing in a rotating field is also used, *i.e.*, continuously changing orientation [37, 38].

(2) Rectangular loop, characterized by a large $K_n \geq 0.9$–0.95. Saturation is achieved in very small fields (of about (1.5–3)H_c), $\mu_i <$ 10 thousand, and $\mu_{max} \geq$ 400 thousand — 1.6 million. Such materials are used in magnetic amplifiers and ferroprobe sensors (such loops are achieved by annealing in a longitudinal magnetic field of 5–12 kE, conducting below the T_C) [39–41].

(3) Linear loops, characterized by high stability of μ_e in the entire range of operating excitation fields (currents) and reaching technical saturation in sufficiently large fields (sometimes greater than 1000 A/m) [42]. Such loops are achieved in three different ways.

• By creating non-magnetic gaps, which complicate the magnetisation process (along the core). The main disadvantage of this method is a significant increase in losses due to flux dissipation in the gap. When using this method of forming a linear loop, saturation is not achieved in large fields and μ_e = const is guaranteed under the action of a direct current biasing field [43, 44].

• By annealing in a transverse magnetic field, during which the external magnetic field is applied perpendicular to the direction of the working magnetic flux (along the width of the ribbon). This creates an induced magnetic anisotropy, which forces the domain structure to orient itself transversely to the excitation, forming an inclined (linear) hysteresis loop with low residual induction. This method allows for obtaining a stable

magnetic permeability and prevents rapid saturation of the material, simulating the effect of a mechanical non-magnetic gap [13, 45].

• Due to the use of thermomechanical processing under a transverse stress, which allows to obtain an induced magnetic anisotropy transverse to the action of the external force (along the ribbon). This processing allows obtaining low values of $\mu_e \approx 1000–1300$; extremely low coercive force; low losses in the core unattainable for cores with a non-magnetic gap [46–49].

Thus, it is the formation of the so-called induced anisotropy, due to the use of thermomechanical processing in a field of a certain direction that allows obtaining the necessary shape of the magnetisation reversal loop for certain compositions of amorphous materials and ensuring the minimisation of energy losses in the core. According to the data presented in Refs. [50, 51], the main contribution to the magnetic anisotropy of amorphous ferromagnets is made by magnetoelastic anisotropy and anisotropy of atomic pairs ordered by orientation (the so-called directional ordering).

3. Magnetic Anisotropy of Ribbon Amorphous Alloys

Let's go into more detail on the nature of magnetism and magnetic anisotropy in amorphous metal alloys. It is known that the source of magnetism is the presence of a magnetic moment that arises due to the intrinsic spin angular momentum of the electron. For spontaneous magnetisation to be possible, atoms must have an internal incomplete $3d$ or $4f$ shell, and the nature of the exchange interaction of spins must be such that the exchange integral is positive [52].

The magnetic-anisotropic state at each point of amorphous alloys is qualitatively characterised by two types of magnetic anisotropy— local and macroscopic ones [53, 54].

I. The presence of local magnetic anisotropy has a weak effect on the magnitude of spontaneous magnetisation, while the T_C decreases. Since in the amorphous state there are local differences in atomic configurations (there is a cluster or nanoinhomogeneous structure), the magnitude of magnetic anisotropy and its direction also differ locally [55, 56].

Magnetisation of amorphous alloys in an external field is carried out by moving the domain boundaries and rotating the spontaneous magnetisation vector [57, 58].

Saturation magnetisation (M_s) for amorphous alloys is usually achieved in fields of 8–80 kA/m. If magnetic anisotropy is absent, then, the so-called circular domain structure is formed, with the domain boundaries having a thickness of about 10 nm. In completely isotropic materials, the circular domain structure leads to the fact that the magnetisation process is carried out not by the movement of the domains (and the domain boundaries do not move over appreciable distances), but exclusively by the rotation of the magnetic moment vectors $\vec{M}_l$ inside the domains [59, 60].

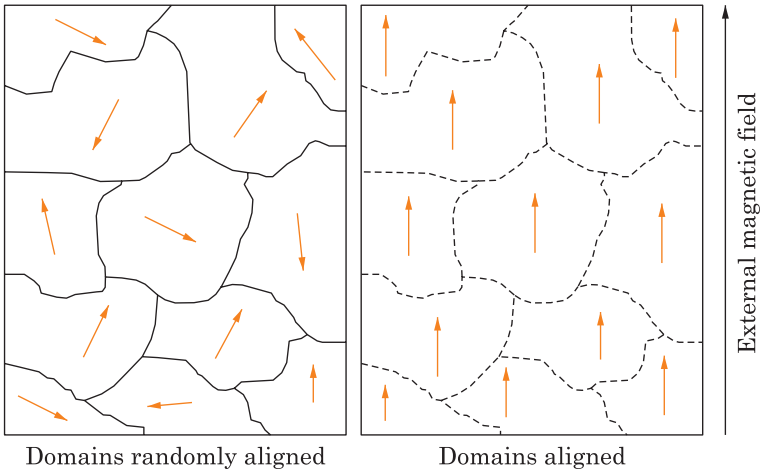

Fig. 5. Schematic representation of ferromagnetic domains in the absence (left) and in the presence (right) of an external magnetic field applied. In the latter case, boundaries are dashed since when domains are aligned (right panel), the sample reaches the saturation point and there are no any domain walls [61]

Easy magnetisation is carried out due to the easily achievable displacement of the domain boundaries and the reverse rotation of the spontaneous magnetisation vector $\vec{M}_s$. In the absence of an external field, the structure is indistinct, but with increasing magnetic field strength (H), the domain walls move in the plane of the ribbon perpendicular to the direction of the field, and the labyrinth structure becomes more distinct. Applying a strong field along the ribbon axis leads to the rotation of the main domain vectors $\vec{M}_s$ and the disappearance of the labyrinth structure. The critical field of such rotation is 8–12 kA/m (this value is close to saturation). Figure 5 reports the schematic view of a ferromagnetic system in absence and in the presence of an external magnetic field applied [61].

The size and nature of the location of the so-called main domains depend on the chemical composition of the alloy and the method of obtaining the tape [60]. The appearance of domains with 180° boundaries corresponds to 'soft' magnetisation, and the main ones to 'hard' magnetisation (*i.e.*, with transversely induced anisotropy, only the so-called main domains should exist). The so-called Barkhausen jumps correspond to the breaking of 180° domain boundaries and indicate the inhomogeneity of the magnetic structure [62].

II. In addition to local magnetic anisotropy, there is also a uniaxial one [63], which is associated with elastic stresses. Magnetoelastic energy [64]

$$E_\sigma = -\frac{3}{2}\lambda_s \cos^2\theta \qquad (3)$$

is a measure of magnetoelastic magnetic anisotropy and depends on the magnetostriction λ_s of the material ($\lambda = \Delta l/l$ + in a magnetic field), l is the length of the tape sample, θ is the angle between the direction of action of tensile stresses (internal or external) and the spontaneous magnetisation vector $\vec{M}_s$. When changing the direction of action of internal stresses, E_σ can change in such a way that these stresses will interfere with the movement of domain boundaries, *i.e.*, cause a decrease in magnetic permeability (μ) and an increase in the coercive force H_c.

The cause of magnetostriction is the dipole interaction between the magnetic moments of electrons, which depends on the interatomic distances and, in amorphous alloys, is determined by disordered atomic configurations [65]. The magnetoelastic effect is the cause of the appearance of magnetic anisotropy and, accordingly, the coercive force (H_c).

The saturation magnetostriction λ_s depends on the chemical composition. For example, $\lambda_s \to 0$ for alloys of the system $(Fe_{1-x}Co_x)_{75}Si_{15}B_{10}$ at $x \to 0.94$, while the domain structure is very weak. Value $\frac{\vec{H}_a \cdot \vec{M}_s}{2}$ represents the energy of magnetic anisotropy associated with the main domains, where $\mathbf{H}_a$ is the magnitude of the field necessary to destroy the main domains. Accordingly, $(\vec{H}_a \cdot \vec{M}_s) \propto \lambda_s$. Thus, the greater the saturation magnetostriction, it is more difficult to induce a certain magnetic anisotropy in the alloy.

The main domains are formed due to the perpendicular component of stresses (tensile or compressive, depending on the sign of the saturation magnetostriction), which leads to the appearance of magnetic anisotropy in the direction of the ribbon thickness [66].

The main domains occupy only part of the ribbon surface. From the outside of the ribbon, they are surrounded by domains with 180° boundaries. It is this domain structure that is the cause of the appearance of hysteresis and coercive force $H_c \approx f(\lambda_s)$ [67].

When there are disordered internal stresses with short wavelengths in the ribbon (*e.g.*, deep frequent cavities or other roughness), magnetostriction has a strong effect on the magnetisation process in weak fields (where the effect is due to the 180° delay of domain boundaries parallel to the ribbon).

III. The coercive force can also increase as a result of magnetocrystalline anisotropy, which is formed in the presence of small (≈10 nm) crystallites in the ribbon (when the cooling rate was insufficient when obtaining an amorphous ribbon or the crystallisation process began during heat treatment) [68].

IV. At the edges of the amorphous ribbon, domains with 180° walls are highly bent. The structure that is formed in this case reflects the flow of molten metal during the ribbon production process. Shear stresses arise, which cause the initially disordered atomic configurations to become ori-

ented along the melt direction. This leads to uniaxial magnetic anisotropy due to the anisotropic distribution of atomic pairs [69, 70]. Stress relaxation leads mainly to a decrease in the coercive force H_c, and an increase in the residual induction B_r (accordingly, $K_n = B_r/B_s$) [71].

V. The magnetic anisotropy induced by annealing in a magnetic field is also uniaxial [72]. The energy of the induced magnetic anisotropy [73]

$$E_u(\theta) = -K_u \cos^2 \theta, \; \Delta S = \int_0^{M_s} Hd(M_1 - M_2). \qquad (4)$$

The constant of the induced magnetic anisotropy K_u depends on the temperature and annealing time of the amorphous alloy. It has been shown that this dependence is smaller, the closer the temperature of thermomagnetic treatment is to the Curie point of the alloy [74]. K_{us} is the corresponding value in saturation depending on T_a.

The appearance of magnetic anisotropy during thermomechanical treatment below T_C is associated with processes that are thermally activated. The reason for this phenomenon is the diffusion of magnetic atoms [67]. K_u obeys the Arrhenius law, and the relaxation time $\tau \; \mu \; 1/T_a$ is from 500 to 10^5 s.

The obtained value of the activation energy of the appearance of anisotropy K_u is of ≈1 eV for amorphous materials, which is 2–3 times smaller than the value for crystalline solid solutions (such as Fe–Si-steels, Ni or Fe–Ni-permalloys). In amorphous materials, as in crystalline materials, the constant of induced magnetic anisotropy increases, when alloys are doped with other magnetic components [67].

Studies of amorphous materials by T. Egami *et al.* [75] revealed changes in the average atomic volume in amorphous alloys during their heat treatment below the temperature of the onset of crystallisation.

Some theories establish a connection between the corresponding microscopic structure and the general (volume) magnetic properties [76, 77]. The most widespread is the theory proposed by G. Kronmüller [78]. To predict macroscopic magnetic properties in an amorphous material, especially those, which have technical significance (these include coercive force, saturation magnetisation (induction), initial permeability, magnetic anisotropy, *etc.*), it is necessary to know the local structure at large distances [67]. Macroscopic (>1 μm) and nanostructured (from 10 to 100 nm) fluctuations in amorphous alloys especially affect [79]: domain structure; domain wall mobility; dynamics of saturation approaching; temperature dependence of magnetisation; magnetostrictive stresses. In turn, it is volume and local magnetic measurements that can provide general information about fluctuations of the atomic structure in amorphous materials at medium distances.

In particular, when studying the bulk magnetic properties of many amorphous materials, G. Kronmüller showed [80] that the nature of ap-

proaching saturation in them is determined by defect structures, since they create elastic stresses, which lead to the emergence of elongated (extended) regions of spin inhomogeneity due to magnetoelastic binding energy.

Kronmüller and Greger [81] concluded that a relatively large contribution to the coercive force of magnetostrictive amorphous materials is provided by the volume pinning of domain walls on defects. In Ref. [82], it was established that there are two types of stresses: short-range stresses that hold the domain walls and long-range stresses that determine the domain structure.

Short-range stresses are determined by quasi-dislocation dipoles with dimensions of 5–300 nm. The appearance of such dipoles can be due to the presence of free volume in the liquid phase, which is partially preserved in the amorphous material [82]. Long-range stresses are due to inhomogeneities fixed in the crystal lattice during ultrafast cooling of the melt.

During quenching from the liquid state, instantaneous coexistence of liquid and solid phases is possible, resulting in regions of compressive and tensile stresses. In amorphous materials, in which the saturation magnetostriction $\lambda_s > 0$, tensile stresses lead to the formation of wide wave-shaped shear bands, and compressive stresses form narrow shear bands with a slight direction perpendicular to the strip surface [67, 83].

Thus, magnetic anisotropy will be induced by annealing in a magnetic field, the easier the lower the alloy magnetostriction [84]. That is why rapidly quenched Co-based alloys, which have almost zero magnetostriction [85], are promising materials for magnetic circuits operating at high frequencies.

It is known [86, 87] that, immediately after obtaining, amorphous alloys demonstrate mainly a low permeability, the magnitude of which significantly depends on the magnitude of the external field. In Ref. [68], it was shown that the positive effect of heat treatment at temperatures above the Curie temperature (T_C) and immediately below the crystallisation temperature (T_x) on the removal of stress introduced by quenching, and the improvement of coercive force and permeability was observed. The authors of Ref. [88] indicated that the formation of residual elastic stresses, secondary phase, defects and dissolved impurities inside nanograins can also increase the coercive force of the soft magnetic matrix phase.

The permeability increases, when the alloys are annealed at a temperature T_a (annealing temperature) between T_C and T_x under the condition $T_C < T_x$ [89, 90]. In case, when the alloys have $T_C > T_x$, *i.e.*, $T_a < T_C$, the permeability does not increase, but, on the contrary, decreases due to the effect of heat treatment without a field, since local magnetic anisotropy is introduced, when annealing below T_C [91]. Amorphous alloys with high magnetic induction are mainly characterised by $T_C > T_x$.

In Ref. [85], it was noted that the metalloid content on the iron content for compositions with zero magnetostriction in the Fe–Co–Cr–Si–B

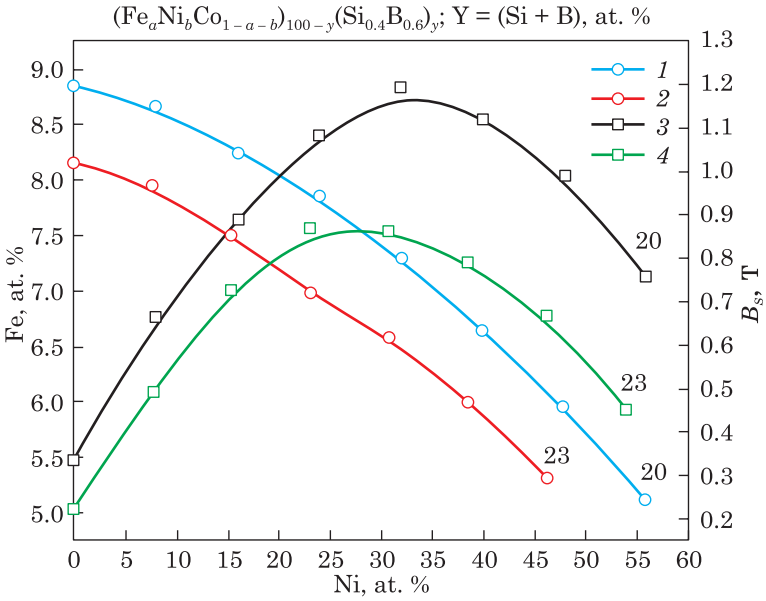

Fig. 6. Dependence of saturation induction B_S in the system $(Fe_aCo_{1-a-b}Ni_b)_{100-y}$ $(Si_{0.4}B_{0.6})_y$ on the Ni content ($0 < b < 0.6$) and the total metalloid content ($y = 20, 23$). Dependence of iron content on Ni content and metalloid content to ensure $\lambda_s = 0$ of the alloy. According to Ref. [92]

system. With an increase in the Ni content, a higher permeability is obtained at the zero magnetostriction line, although the saturation magnetisation decreases [92]. The absolute values of compositions with zero magnetostriction (λ_s) are known for alloys based on the Fe–Co–Ni system [93]. In Ref. [94], it was shown that the zero magnetostriction line shifts with a change in the metalloid content. As shown in Ref. [92], the compositions with zero magnetostriction, magnetic properties and crystallisation temperatures T_x in the system $(Fe_aCo_{1-a-b}Ni_b)_{100-y}(Si_{0.4}B_{0.6})_y$ as a function of the Ni content ($0 < b < 0.6$) and the metalloid content ($20 < y < 30$) were considered. The iron content in the composition with zero magnetostriction in this system increases with decreasing metalloid content (y) and increasing Ni content ($b \le 0.4$) (Fig. 6), as well as decreasing Si/(Si+B) ratio. The dependence of iron content on metalloid content is more sensitive to increasing Ni content. The weak uniaxial anisotropy along the ribbon axis, which is introduced during quenching, significantly affects the properties in a weak field. After annealing at $T_a < T_C$, a shifted B–H loop was observed for a ribbon toroidal core for an alloy with high induction. After annealing at $T_C < T_a < T_x$, alloys with high magnetic permeability (μ_i) and relatively low coercive force and residual induction (B_r) were obtained [95].

However, the main disadvantage of such amorphous materials is that for alloys with high saturation induction B_s = 0.9–1.1 T, the Curie temperature is higher than the crystallisation temperature (T_x), which does not allow us to count on an effective influence on the shape of the hysteresis loop of thermomagnetic treatment [87, 96].

It is known [97] that the magnetic properties of amorphous alloys can be significantly improved by annealing in a magnetic field of a certain direction. The rule of thumb is that to achieve the most positive result, such annealing should be carried out in the immediate vicinity of the Curie temperature (T_C) (slightly below this temperature).

It has been shown [98] that the addition of manganese to alloys of the Co–Fe–Si–B system is very useful, since it expands the temperature range ($T_x - T_C$) of amorphous alloys without reducing magnetic induction. At a manganese concentration of up to 4 at.%, the crystallisation temperature T_x remains practically unchanged, whereas the Curie temperature (T_C) decreases with increasing manganese content [98]. This allows annealing at temperatures above T_C without the risk of crystallisation. In Ref. [99], it was shown that in alloys of the Co–Mn–B system, the effect of manganese on magnetisation depends on the boron content. The presence of manganese shifts the Co/Fe ratio to provide saturation magnetostriction ($\lambda_s = 0$) to a higher value [98].

The temperature dependences of the effective permeability μ/μ_{20} obtained in Ref. [100] for samples of amorphous ribbons of the $Co_{70}Fe_5Si_{15}B_{10}$ alloy have a look typical of systems, in which the processes of stabilisation and destabilisation of domain boundaries occur upon heating. In each case, the effective magnetic permeability μ_e (μ/μ_{20}) except for a small temperature range (up to 60–120 °C) first decreases with increasing temperature (stabilisation of domain boundaries), and then, having passed the minimum, increases (destabilisation of domain boundaries). Near the T_C for alloys of this type with zero magnetostriction, a Hopkinson-type maximum is observed. According to the data presented in Ref. [91], the stabilisation of domain boundaries occurs because of atomic compositional directional ordering stimulated by the gain of the magnetic component of free energy. The increase in the effective magnetic permeability (μ_e), when heated above 250 °C, may be associated with structural relaxation, which is accompanied by the release of free volume [91].

The decrease in the degree of stabilisation of domain boundaries for alloys enriched in manganese and depleted in nickel occurs due to the slower compositional ordering of pairs of basic magnetic atoms [68]. After reaching the maximum, a sharp decline occurs, which indicates an approach to the paramagnetic state of the system (attainment of the Curie temperature). In addition, a rather sharp drop in the relative magnetic permeability, as noted in Ref. [101] for the saturation magnetisation of the $Co_{70}Fe_5Si_4B_{16}$ alloy with $T_C > T_x$, may be associated with the development of primary crystallisation processes.

The Curie temperature (T_C), as well as the crystallisation temperature (T_x), is noticeably reduced for alloys with high nickel content and low manganese [102, 103]. Establishing the temperature intervals of crystallisation and Curie temperatures, as well as the course of the temperature dependences μ/μ_{20}, allows you to correctly select the temperatures for treating alloys of different chemical compositions to ensure maximum efficiency of thermomagnetic treatment.

According to the data presented in Ref. [92], the simplest transverse anisotropy is formed in alloys with a high nickel and iron content, which is obviously associated with more complex processes of redistribution of components in the strip.

As a result of studying the influence of thermomagnetic treatment, it was found that the magnetic properties of the cores strongly depend on the chemical composition of the alloy and the annealing temperature [85, 92]. From the point of view of practical use, alloys with maximum magnetic permeability (after longitudinal thermomagnetic treatment) of 600 and 1500 thousand are promising [104, 105]. It is such alloy compositions, which can compete successfully with permalloy magnetic cores with high magnetic permeability (μ_{max}) [106]. Magnetic cores from alloys with high μ_{max} can be effectively used in modern electromagnetic and high-frequency devices, in particular, in electromagnetic relays with improved switching dynamics, energy-efficient common-mode inductors and medium- and high-frequency transformers [107].

4. Anisotropy and Disaccommodation of Ribbon Amorphous Alloys

In amorphous soft magnetic alloys, the magnetic after-effects are clearly expressed, which are caused by the stabilisation of domain boundaries due to directional ordering. The theory of domain boundary stabilisation and its influence on magnetic properties was developed for crystalline materials [68]. However, the main ideas and conclusions from this theory are also used to describe the behaviour of amorphous soft magnetic alloys when introducing local (in the volume of domain boundaries and individual domains) and macroscopic uniaxial anisotropy [108, 109].

Ideally, in a completely isotropic magnet, domain walls should be absent, and magnetic moments should rotate freely throughout the entire volume of the sample. However, in real amorphous materials, as noted above, there are clear 180° walls that determine their properties, such as magnetic permeability, coercive force, or Barkhausen jumps during magnetisation [110, 111].

The anisotropy induced by annealing or thermomagnetic treatment is also characterised by second-order symmetry and reversibility upon repeated thermal treatments [112, 113].

It turned out [114] that neither magnetostrictive stresses nor internal shape effects can explain the obtained result, since the dependence $K_u(x)$ is

radically different from the dependences $\lambda_s(x)$ and $M_s^2(x)$. Moreover, the value of the constant of the induced magnetic anisotropy K_u does not change significantly after thermal treatment at sufficiently high temperatures. Interestingly, the value of the anisotropy remains approximately constant after crystallisation of the sample as a result of annealing at a higher temperature or for a longer duration. This may be associated [115] with the presence of microcrystals in the rapidly quenched ribbon. Since even a weak orientation of these in an amorphous matrix can lead to anisotropy.

When amorphous alloys are cooled in a magnetic field, uniaxial magnetic anisotropy is observed. For most amorphous alloys, the value of the constant of such anisotropy ranges from 10 to 10^3 J/m^3 and coincides in order of magnitude with its value for magnetically disordered crystalline alloys [116].

The magnetic after-effect was studied on the example of amorphous materials of various systems [108, 109, 117, 118], including amorphous soft magnetic alloys that do not contain metalloid atoms [117, 118]. It was proved that the magnetic after-effect cannot be eliminated by annealing [106, 117, 118], since in amorphous materials it is not associated with the presence of metalloid atoms, but is a consequence of the evolution of the atomic structure of the amorphous phase [67].

One of the characteristic manifestations of the stabilisation of domain boundaries due to directional ordering is the magnetoreversible time decay of the initial permeability. Since the initial permeability μ decreases with time after demagnetisation, but because of repeated demagnetization, it is restored to the initial level. The processes of directional ordering and the associated stabilisation of domain boundaries in amorphous materials occur at temperatures close to room temperature [119].

In a number of works [120–122], the properties of the time decay of permeability in amorphous soft magnetic alloys were studied. It was shown [121, 122] that the magnitude of the time decay of permeability significantly depends on the nature of the initial magnetic texture of amorphous materials, which, in turn, can be created in one of the following ways: by varying the conditions for obtaining the tape (cooling rate [120]; annealing in a magnetic field or under stress [123]). There are also attempts to relate the magnitude of the temporal decrease in permeability to saturation magnetostriction [124].

The results presented in Ref. [67] indicate that the magnetic after-effect can change the following parameters of the hysteresis loop by more than 50%: reduce the initial and maximum permeability; increase the coercive force; increase the area of the hysteresis loop; and increase the anisotropy energy.

According to the data presented in Ref. [125], there are two types of magnetic after-effect. The first one includes irreversible ones, which are associated with the thermally activated process of microscopic Barkhausen

jumps. The second one includes reversible ones, which are caused by a local increase in the domain wall potential due to the reorganisation of the atomic structure in its volume. It is the second type of magnetic after-effect that affects the operational characteristics of amorphous alloys.

To study the phenomena of magnetic after-effect, the most useful and simple method is the disaccommodation (DA) method (disaccommodation is the change in magnetic permeability over time at a certain constant temperature T: $DA = 100(\mu_T - \mu_t)/\mu_T$) [126].

The magnetic after-effect for most amorphous materials is attributed to the stabilisation of the domain structure as a result of the formation or change in the magnetic field-induced magnetic anisotropy constant K_u. It has been established [127] that the relaxation time spectrum during disaccommodation is very wide, which indicates a large number of atomic configurations that participate in this process. Doping alloys with different elements can reduce disaccommodation [128]. The time dependence of the magnetic permeability (μ) is significantly affected by the parameters of the spinning process [129] and the kinetics of stress relaxation [130].

Practically promising amorphous soft magnetic alloys with zero magnetostriction have been studied quite extensively [131–135]. The 'base' alloy $Fe_5Co_{70}Si_{15}B_{10}$ has been studied in quite detail [136, 137]. It has been shown [137] that, in the case, when the crystallisation temperature T_x is above the Curie point T_C, high values of the initial permeability can be obtained at annealing temperatures $T_a > T_C$ with subsequent rapid cooling. Such treatment provides: a special structural state of the amorphous matrix, which leads to a sharp increase in the mobility of domain boundaries; suppression of the processes of stabilisation of domain boundaries due to directional compositional ordering. However, the specified heat treatment causes a number of negative phenomena [132]: embrittlement, an increase in the temperature-time instability of the initial magnetic permeability, and the need for sufficiently rapid cooling.

In work [131], it was shown that the introduction of nickel instead of cobalt in alloys of the type (Fe, Co, Ni, Si, B) reduces the effect of stabilisation of domain boundaries on the magnetic properties in an alloy with a relatively low Curie point. In the works [138, 139], the effect of preliminary annealing on the magnitude of the induced anisotropy and the nature of the domain structure of the $Fe_5Co_{58}Ni_{10}Si_{11}B_{16}$ alloy was investigated. A detailed study of the coercive force H_c of this alloy was carried out in the work [140], which showed that annealing below the Curie temperature (T_C) causes growth, and high-temperature annealing keeps the coercive force (H_c) practically unchanged.

In ferromagnets, even when the external magnetic field is zero, anisotropic configurations of atomic pairs appear [141, 142]. Their appearance occurs due to diffusion, the driving force of which is the internal magnetic field. This field is associated with the domain structure and, there-

fore, exists even when the external magnetic field is absent. Since the direction of the internal magnetic field (spontaneous magnetisation) for different domains is different, a corresponding distribution of atomic pairs in different domains occurs. That is why [67] there are conditions when the uniaxial anisotropy has a direction characteristic of each domain; otherwise, in amorphous materials, it is possible to create magnetic anisotropy that locally differs in direction.

In addition, within the domain boundaries themselves, new atomic configurations are also stabilised in accordance with the direction of the magnetic moment vectors of atoms in the boundary layer. As a result, the potential energy of the domain boundaries decreases, and they stabilise in their positions [143]. Stabilisation of domain boundaries is nothing more than an increase in the coercive force.

In work [91], using the example of the $Fe_5Co_{58}Ni_{10}Si_{11}B_{16}$ alloy, it was shown that the decrease in $\Delta\mu/\mu$ occurs at annealing temperatures $T_a < 150$ °C, and, at higher annealing temperatures, the value of $\Delta\mu/\mu$ remains practically constant. Both patterns (decrease in $\Delta\mu/\mu$ and unrelaxed μ_a) cannot be associated with structural changes in the amorphous matrix that accompany the process of leaving the residual free volume, since this process develops at higher temperatures ($T \approx 250$ °C) [144, 145]. These patterns are also not associated with the relaxation of internal stresses, since a change in their level should lead to an increase in μ_a. In the work [121], it was shown that the magnitude of the temporal decrease in permeability strongly depends on the nature of the domain structure. It is maximal when the structure is a plane-parallel domain with the vector $\mathbf{I}_s$ coinciding with the sample axis. On the other hand, as was established in the work [139], at annealing temperatures $T_a < T_C$ (150 and 175 °C), in the alloy $Fe_5Co_{58}Ni_{10}Si_{11}B_{16}$, a reorganisation of the domain structure was observed, which the authors associate with a change in the sign of the magnetostriction λ_s. After such annealing, narrow striped domains appear along the 180° domain boundaries parallel to the sample axis, reflecting the appearance of a domain structure associated with the normal component of the Is vector in regions with still unrelieved stresses. This should lead to a decrease in the value of $\Delta\mu/\mu$ [121].

Based on the previously developed model of randomly distributed internal stresses, which takes into account the influence of the value of the constant of the initial magnetic anisotropy and the direction of the easy magnetization axis [146, 147], it is possible to calculate the dependence of the value of the time decay of permeability on the following factors: reduced and initial macroscopic magnetic anisotropy; magnetostriction; rectangularity of the hysteresis loop; parameters of internal stresses. For an analytical solution to the problem of describing the time decay of permeability, a theoretical approach is used, which reduces the influence on the magnetic properties of the chemical composition, the method of produc-

tion and various treatments of amorphous alloys to changes in the parameters of magnetic anisotropy in the material.

To calculate the time decay of permeability, the relative change in the initial permeability over a time interval t after demagnetisation was approximated using thin domain boundaries [148]. It is assumed that the thickness of the domain boundaries D is much smaller than the wavelength of spatial fluctuations of the specific energy of the boundary g_R.

The value of μ is determined by 180° displacement of the domain boundaries and described by the expression [68]

$$\mu = 4\mu_0 M_s^2 \cos^2 \varphi_0 \,/\, (\alpha D), \tag{5}$$

where $\mu_0 = 4 \cdot 10^{-7}$ H/m is the magnetic constant; M_s is the saturation magnetization; φ_0 is the angle between the magnetization vector and the magnetic field; $\alpha \equiv (d^2g/dx^2)$ is the stiffness coefficient of the domain boundaries, which is equal to the second derivative of the specific energy of the boundaries along the displacement coordinate at the point of the equilibrium position of the boundary; D is the width of the domains.

After demagnetisation, the domain boundaries fall into new positions, where they stabilise again; their energy decreases by the magnitude of the after-effect potential, because of which their stiffness coefficient increases [68]:

$$\alpha = \alpha(0) + \alpha_s = \alpha(0) + 2p^2K_u/d, \tag{6}$$

where $\alpha(0) = (d^2g_R/dx^2)$ is the unrelaxed value of the stiffness coefficient (at the initial time); $\alpha_s = (d^2g_s/dx^2)$ is the contribution to the stiffness coefficient due to the stabilization of the domain faces due to directional ordering; K_u is the constant of the reduced uniaxial magnetic anisotropy.

From Eqs. (5) and (6), it follows that

$$\Delta\mu/\mu = 1 - [\alpha(0)/\alpha] = [1 + \alpha(0)/\alpha_s]^{-1}. \tag{7}$$

Using Eq. (6), we obtain:

$$\Delta\mu/\mu = 1 - [\alpha(0)/\alpha] = [1 + \alpha(0)\, d/2p^2K_u]^{-1}. \tag{8}$$

Because of directional ordering, all domain boundaries (DB) are stabilized, but not all boundaries contribute to the value of the time decay of permeability, but only those that are displaced in the external field [149]. Within the framework of the biaxial scheme of the magnetic-anisotropic state, this can be formulated as follows: the time decay of permeability is due to the displacement of the DB in longitudinally magnetized regions ($\varphi = 0, \pi$); in transversely magnetized regions ($\varphi = \pm\pi/2$), magnetization is carried out by rotating the magnetization vectors inside the domains and, accordingly, the stabilization of domain boundaries in these regions does not affect the value of the time-dependent permeability.

5. Conclusions

A comprehensive analysis of the magnetic properties of amorphous strip metal materials has been carried out. Particular attention is paid to the mechanisms of magnetic anisotropy formation, the role of thermal and thermomagnetic treatments, as well as relaxation processes that determine the temporal stability of magnetic characteristics.

The main causes of magnetic anisotropy in amorphous ribbon alloys have been analysed, among which the magnetoelastic anisotropy caused by internal stresses and magnetostriction, as well as the anisotropy of directional ordering of atomic pairs, play a decisive role.

It is shown that:

• the formation of magnetic anisotropy is a thermal activation process;

• the driving force of the process of magnetic anisotropy formation is the interatomic magnetic interaction;

• the process of anisotropy induction proceeds much faster and the energy of magnetic anisotropy is achieved higher in amorphous materials containing two or more metals.

Acknowledgements. This work was carried out as part of the research work 'Structural and phase states and physical and mechanical properties of precision Co–Ni–Cr and Ni–TiC superalloys and protective coatings based on them for the machine-building and energy industries' (2025–2029) (State Reg. No. 0124U002939).

Authors' Contributions

V.K.N.: supervision of the research, formulation of the main ideas, providing the manuscript structure, and important comments on the final text. All other authors (V.V.K., B.S.B., I.K.Ye., A.V.N., V.E.Ia, M.S.N., and V.A.D.) performed a critical analysis of the literature and contributed equally to the writing of each section. All authors approved the final version of the manuscript.

REFERENCES

1. V.A. Dekhtyarenko, V.K. Nosenko, V.V. Kyrylchuk, A.V. Nosenko, O.M. Semyrga, I.K. Yevlash, and V.I. Bondarchuk, Amorphous Alloys as a Promising Class of Functional Materials. Pt. 1: Manufacturing Methods, Structure, Physical and Mechanical Properties, *Prog. Phys. Met.*, **26**, No. 3: 598–625 (2025); https://doi.org/10.15407/ufm.26.03.598
2. B.S. Baitalyuk, V.K. Nosenko, I.K. Yevlash, A.V. Nosenko, V.E. Iakovlev, and V.A. Dekhtyarenko, Powder Soft Magnetic Composites: Problems and Prospects, *Prog. Phys. Met.*, **27**, No. 1: 50–83 (2026); https://doi.org/10.15407/ufm.27.01.050
3. I.S. Miroshnichenko and I.V. Salli, A Device for the Crystallization of Alloys at a High Cooling Rate, *Ind. Lab.*, **25**, No. 11: 1463–1464 (1959).
4. P. Duwez, R.H. Willens, and W. Klement, Continuous Series of Metastable Solid Solutions in Silver–Copper Alloys, *J. Appl. Phys.*, **31**: 1136–1137 (1960); https://doi.org/10.1063/1.1735777

5. A.L. Greer, Metallic Glasses, *Science*, **267**, No. 5206: 1947–1953 (1995); https://doi.org/10.1126/science.267.5206.1947
6. A. Inoue, Stabilization of Metallic Glassy Liquids, *Acta Mater.*, **48**, No. 1: 279–306 (2000); https://doi.org/10.1016/S1359-6454(99)00300-6
7. J.F. Löffler, Bulk Metallic Glasses, *Intermetallics*, **11**, No. 6: 529–540 (2003); https://doi.org/10.1016/S0966-9795(03)00046-3
8. W.H. Wang, C. Dong, and C.H. Shek, Bulk Metallic Glasses, *Mater. Sci. Eng. R Rep.*, **44**, No. 2–3: 45–139 (2004); https://doi.org/10.1016/j.mser.2004.03.001
9. A. Takeuchi and A. Inoue, Calculations of Mixing Enthalpy and Mismatch Entropy for Ternary Amorphous Alloys, *Mater. Trans., JIM*, **41**: 1372–1378 (2000); https://doi.org/10.2320/matertrans1989.41.1372
10. A. Takeuchi and A. Inoue, Classification of Bulk Metallic Glasses by Atomic Size Difference, Heat of Mixing and Period of Constituent Elements and its Application to Characterization of the Main Alloying Element, *Mater. Trans., JIM*, **46**: 2817–2829 (2005); https://doi.org/10.2320/matertrans.46.2817
11. J.M. Silveyra, E. Ferrara, D.L. Huber, and T.C. Monson, Soft Magnetic Materials for a Sustainable and Electrified World, *Science*, **362**, No. 6413: 418 (2018); https://doi.org/10.1126/science.aao0195
12. W. Wang, J. Fan, C. Li, Y. Yu, A. Wang, S. Li, and J. Liu, Low-Loss Soft Magnetic Materials and Their Application in Power Conversion: Progress and Perspective, *Energies*, **18**, No. 3: 482 (2025); https://doi.org/10.3390/en18030482
13. M. Nie, C. Jiang, Y. Yang, B. Zhou, Z. Chen, G. Jia, Z. Li, C. Dai, J. He, and H. Guo, Multicomponent Soft Magnetic Alloys for Soft Magnetic Composites: A Review, *Mater. Today Electron.*, **12**: 100153 (2025); https://doi.org/10.1016/j.mtelec.2025.100153
14. Z. Feng, H. Geng, Y. Zhuang, and P. Li, Progress, Applications, and Challenges of Amorphous Alloys: A Critical Review, *Inorganics*, **12**, No. 9: 232 (2024); https://doi.org/10.3390/inorganics12090232
15. L. Novák, J. Kováč, and B. Kunca, Study of Magnetization Processes in Amorphous Ferromagnetic Alloys after Heat Treatment below the Crystallization Temperature, *J. Non-Cryst. Solids*, **637**: 123041 (2024); https://doi.org/10.1016/j.jnoncrysol.2024.123041
16. Si. Yamaura, W. Zhang, and A. Inoue, Introduction to Amorphous Alloys and Metallic Glasses, *Novel Structured Metallic and Inorganic Materials* (Eds. Y. Setsuhara, T. Kamiya, Si Yamaura) (Springer: 2019), p. 3–22; https://doi.org/10.1007/978-981-13-7611-5_1
17. X.S. Li, F.C. Su, J. Zhou, Y.C. Mao, J.M. Yang, Z.Y. Xue, H.Y. Sohrabi, and W.H. Wang, Ductile Fe-Based Amorphous Alloy with Excellent Soft Magnetic Properties Induced by Low-Temperature Stress Annealing, *Intermetallics*, **166**, 108201 (2024); https://doi.org/10.1016/j.intermet.2024.108201
18. S. Lesz, P. Kwapuliński, M. Nabiałek, P. Zackiewicz, and L. Hawelek, Thermal Stability, Crystallization and Magnetic Properties of Fe–Co-Based Metallic Glasses, *J. Therm. Anal. Calorim.*, **125**: 1143–1149 (2016); https://doi.org/10.1007/s10973-016-5430-x
19. J. Qiao, P. Yu, Y. Wu, T. Chen, Y. Du, and J. Yang, A Compact Review of Laser Welding Technologies for Amorphous Alloys, *Metals*, **10**, No. 12: 1690 (2020); https://doi.org/10.3390/met10121690

20. J. Kang, X. Yang, Q. Hu, Z. Cai, L.-M. Liu, and L. Guo, Recent Progress of Amorphous Nanomaterials, *Chem. Rev.*, **123**, No. 13: 8859–8941 (2023); https://doi.org/10.1021/acs.chemrev.3c00229
21. A. Sharma, V.Yu. Zadorozhnyy, J. Wenrui, and J.C. Qiao, Review of Thermo-Mechanical Processing of Metallic Glasses, *J. Non-Cryst. Solids*, **666**, 123714 (2025); https://doi.org/10.1016/j.jnoncrysol.2025.123714
22. A.L. Greer, Metallic Glasses, *Physical Metallurgy* (Eds. D.E. Laughlin and K. Hono) (Elsevier: 2014), p. 305–385; https://doi.org/10.1016/B978-0-444-53770-6.00004-6
23. S. Mathias, C. La-O-Vorakiat, P. Grychtol, and H.C. Kapteyn, Probing the Timescale of the Exchange Interaction in a Ferromagnetic Alloy, *PNAS*, **109**, No. 13: 4792–4797 (2012); https://doi.org/10.1073/pnas.1201371109
24. F. Cardarelli, Magnetic Materials, *Materials Handbook* (Springer: 2018), p. 737–775; https://doi.org/10.1007/978-3-319-38925-7_7
25. A. Chrobak, G. Haneczok, P. Kwapuliński, D. Chrobak, Z. Stokłosa, and J. Rasek, Soft Magnetic Properties of the $Fe_{72}Co_{10}Nb_6B_{12}$ Amorphous Alloy, *J. Alloys Compd.*, **423**: 77–80 (2006); https://doi.org/10.1016/j.jallcom.2005.12.050
26. Z. Zhang, Z.D. Zhang, Y.F. Cai, Y. Zhang, Y. Wu, H.H. Zhu, Y.Y. Qian, Y.E. Zhang, Y.C. Wang, Y.Q. Yan, X. Tong, B. Zhang, C. Yang, H.B. Ke, H.Y. Bai, and W.H. Wang, A Unique Fe-Based Soft Magnetic Alloy and its Magnetic Softening Mechanism, *J. Alloys Compd.*, **1002**: 175161 (2024); https://doi.org/10.1016/j.jallcom.2024.175161
27. Z. Li, W. Han, Z. Xin, Q. Liu, and J. Chen, A Review of Magnetic Core Materials, Core Loss Modeling and Measurements in High-Power High-Frequency Transformers, *CPSS Trans. Power Electron. Appl.*, **7**, No. 4: 359–373 (2022); https://doi.org/10.24295/CPSSTPEA.2022.00033
28. J. Zhang, Y. Qin, X. Liu, Y. Zhao, W. Dang, X. Fan, X. Chen, Y. Yu, Z. Yang, S. Gao, D. Wu, and Y. Fang, Stress-Induced Magnetic Anisotropy in Fe-Based Amorphous/Nanocrystalline Alloys: Mechanisms, Advances and Challenges, *Materials*, **18**, No. 7: 1499 (2025); https://doi.org/10.3390/ma18071499
29. M.F. Campos and J. De Castro, Comparative View of Coercivity Mechanisms in Soft and Hard Magnetic Materials, *Arch. Electr. Eng.*, **73**, No. 4: 1087–1101 (2024); https://doi.org/10.24425/aee.2024.152112
30. H.Z.A. Hein, S. Yue, and Y. Li, Comparative Core Loss Calculation Methods for Magnetic Materials under Harmonics Effect, *IOP Conference Series: Mater. Sci. Eng.*, **486**: 012019 (2019); https://doi.org/10.1088/1757-899X/486/1/012019
31. C.W.T. McLyman, *Transformer and Inductor Design Handbook* (CRC Press: 2011); https://doi.org/10.1201/b10865
32. S.D. Sudhoff, Magnetic Core Loss and Material Characterization, *Power Magnetic Devices: A Multi-Objective Design Approach*, 2nd Edition, (Wiley-IEEE Press: 2021), Ch. 6, p. 257–293; https://doi.org/10.1002/9781119674658.ch6
33. M.E. McHenry, M.A. Willard, and D.E. Laughlin, Amorphous and Nanocrystalline Materials for Applications as Soft Magnets, *Prog. Mater. Sci.*, **44**, No. 4: 291–433 (1999); https://doi.org/10.1016/S0079-6425(99)00002-X

34. F. Mazaleyrat, Soft Magnetic Materials and Applications, in: *Handbook of Magnetism and Magnetic Materials*, (Eds. J.M.D. Coey and S.S.P. Parkin) (Springer: 2021), p. 1435–1487;
https://doi.org/10.1007/978-3-030-63210-6_31
35. M. Kazimierczuk, Magnetic Cores, *High-Frequency Magnetic Components*, (Wiley: 2013), Ch. 2, p. 81–162;
https://doi.org/10.1002/9781118717806.ch2
36. M. Şahin, Inductance Selection Criteria and Design Steps for Power Electronics Applications, *Süleyman Demirel Üniv. Fen Bilim. Enst. Derg.*, **24**, No. 3: 689–695 (2020);
https://doi.org/10.19113/sdufenbed.543986
37. N. Ito and K. Suzuki, Improvement of Magnetic Softness in Nanocrystalline Soft Magnetic Materials by Rotating Magnetic Field Annealing, *J. App. Phys.*, **97**, 10F503 (2005);
https://doi.org/10.1063/1.1854255
38. L. Shao, R. Bai, Y. Wu, J. Zhou, X. Tong, H. Peng, T. Liang, Z. Li, Q. Zeng, B. Zhang, H. Ke, and W. Wang, Critical State-Induced Emergence of Superior Magnetic Performances in an Iron-Based Amorphous Soft Magnetic Composite, *Mater. Futures*, **3**: 025301 (2024);
https://doi.org/10.1088/2752-5724/ad2ae8
39. W. Zheng, G. Zhang, Q. Zhang, H. Yu, Z. Li, M. Gu, S. Song, S. Zhou, and X. Qu, The Effect of Annealing on the Soft Magnetic Properties and Microstructure of $Fe_{82}Si_2B_{13}P_1C_3$ Amorphous Iron Cores, *Materials*, **16**, No. 16: 5527 (2023);
https://doi.org/10.3390/ma16165527
40. M. Jiang, J. Wang, M. Cai, J. Li, W. Dong, Z. Guo, and B. Shen, Improvement of Soft Magnetic Properties for Fe-Based Amorphous/Nanocrystalline Alloy by Longitudinal Magnetic Field Annealing, *J. Non-Cryst. Solids*, **650**: 123382 (2025);
https://doi.org/10.1016/j.jnoncrysol.2024.123382
41. Y. Yin, C. Cheng, F. Kong, W. Yang, X. Lin, S. Yue, and A. Wang, Dynamic Magnetic Characteristics and Their Dependences on Servicing Conditions of Fe-Based Nanocrystalline Alloy Cores Modulated *via* Transverse Magnetic Field Annealing, *IEEE Trans. Magn.*, **61**, No. 12: 2001308 (2025);
https://doi.org/10.1109/TMAG.2025.3626790
42. V.K. Nosenko, V.V. Maslov, A.P. Kochkubey, and V.V. Kirilchuk, New Soft Magnetic Amorphous Cobalt Based Alloys with High Hysteresis Loop Linearity, *J. Phys.: Conf. Ser.*, **98**: 072006 (2008);
https://doi.org/10.1088/1742-6596/98/7/072006
43. M. Kim, M. Lee, S. Lee, J. Lee, and J. Song, B–H Curve Estimation and Air Gap Optimization for High-Performance Split Core, *Materials*, **18**, No. 3: 644 (2025);
https://doi.org/10.3390/ma18030644
44. F. Battal, A Comparative Analysis of Core Material and Gap Sizing Effect on the High-Power Inductor Design, *Eng. Sci. Technol., Int. J.*, **63**: 102001 (2025);
https://doi.org/10.1016/j.jestch.2025.102001
45. C. Mu, Q. Ding, L. Pan, H. Ma, M. Su, Z. Tian, A. He, Y. Dong, D. Li, Q. Man, and J. Li, Effect of Transverse Magnetic Annealing on the Surface Texture and Magnetization Process of FeSiBNbCuP Nanocrystalline Alloys, *J. Magn. Magn. Mater.*, **630**, 173461 (2025);
https://doi.org/10.1016/j.jmmm.2025.173461
46. A. Nosenko, T. Mika, O. Rudenko, Y. Yarmoshchuk, and V. Nosenko, Soft Magnetic Properties of Nanocrystalline $Fe_{73}B_7Si_{16}Nb_3Cu_1$ Alloy After Rapid Heating Under Tensile Stress, *Nanoscale Res. Lett.*, **10**: 136 (2015);
https://doi.org/10.1186/s11671-015-0837-z

47. A. Nosenko, T. Mika, O. Semyrga, and V. Nosenko, Effect of Mechanical Stresses in Rapidly Heated $Fe_{73}Cu_1Nb_3Si_{16}B_7$ Ribbon Arising During the Ring Core Formation on Their Magnetic Properties, *Nanoscale Res. Lett.*, **12**: 299 (2017); https://doi.org/10.1186/s11671-017-2041-9
48. R. Parsons, K. Onodera, H. Kishimoto, T. Shoji, A. Kato, and K. Suzuki, Effect of Tensile Stress During Ultra-Rapid Annealing on the Soft Magnetic Properties of Fe-B Based Nanocrystalline Alloys, *J. Alloys Compd.*, **924**: 166374 (2022); https://doi.org/10.1016/j.jallcom.2022.166374
49. N.M. Bruno, A.K. Dey, S.P.S. Badheka, and V.S. Gopinath, A New High-Toughness Co-Based Nanocrystalline Soft-Magnetic Alloy Capable of Large Stress-Induced Anisotropy, *Scripta Mater.*, **271**: 116998 (2025); https://doi.org/10.1016/j.scriptamat.2025.116998
50. R.C. O'Handley, *Modern Magnetic Materials: Principles and Applications* (Wiley: 2000).
51. M.G. Nematov, I. Baraban, N.A. Yudanov, V. Rodionova, F.X. Qin, H.-X. Peng, and L.V. Panina, Evolution of the Magnetic Anisotropy and Magnetostriction in Co-Based Amorphous Alloys Microwires Due to Current Annealing and Stress-Sensory Applications, *J. Alloys Compd.*, **837**: 15584 (2020); https://doi.org/10.1016/j.jallcom.2020.155584
52. N.A. Spaldin, Atomic Origins of Magnetism, in *Magnetic Materials: Fundamentals and Applications* (Cambridge University Press: 2010), p. 22–37; https://doi.org/10.1017/CBO9780511781599.003
53. R. Alben, J.J. Becker, and M.C. Chi, Random Anisotropy in Amorphous Ferromagnets, *J. Appl. Phys.*, **49**, No. 3: 1653–1658 (1978); https://doi.org/10.1063/1.324881
54. S. Stambuła, K. Jez, M. Major, R.M. Said, P. Vizureanu, M. Nabialek. and B. Jez, Research on Magnetic Anisotropy in Amorphous Materials with Soft Magnetic Properties, *Acta Phys. Pol. A*, **147**, No. 3: 162–164 (2025); https://doi.org/10.12693/APhysPolA.147.162
55. Y. Elsässer, M. Fähnle, E.H. Brandt, and M.C. Böhm, Theory of Local Magnetic Anisotropy in Amorphous Alloys, *J. Phys. F: Metal Phys.*, **18**, No. 11: 2153 (1988); https://doi.org/10.1088/0305-4608/18/11/018
56. G. Herzer, *The Random Anisotropy Model*, in: *Properties and Applications of Nanocrystalline Alloys from Amorphous Precursors* (Eds. B. Idzikowski, P. Švec, and M. Miglierini) (NATO Science Series: 2005), **184**, p. 15–34; https://doi.org/10.1007/1-4020-2965-9_2
57. N.N. Orlova A. S. Aronin, S.I. Bozhko, Yu.P. Kabanov, and V.S. Gornakov, Magnetic Structure and Magnetization Process of the Glass-Coated Fe-Based Amorphous Microwire, *J. Appl. Phys.*, **111**: 073906 (2012); https://doi.org/10.1063/1.3702448
58. S. Stambuła, M. Nabiałek, P. Paszta, M.M. Nabiałek, P. Pietrusiewicz, F. Somidin, and B. Jeż, Process of Magnetization in Strong Magnetic Fields of Amorphous Fe-Based Alloys, *Acta Phys. Pol. A*, **147**, No. 3: 168 (2025); https://doi.org/10.12693/APhysPolA.147.168
59. I. Betancourt, G. Hrkac, and T. Schrefl, Micromagnetic Study of Magnetic Domain Structure and Magnetization Reversal in Amorphous Wires with Circular Anisotropy, *J. Magn. Magn. Mater.*, **323**, No. 9: 1134–1139 (2011); https://doi.org/10.1016/j.jmmm.2010.11.089
60. M. Takezawa, Magnetic Domain Structures. *Handbook of Magnetic Material for Motor Drive Systems* (Ed. K. Fujisaki) (Springer: 2025); https://doi.org/10.1007/978-981-96-5701-8_14
61. R. Nisticò, F. Cesano, and F. Garello, Magnetic Materials and Systems: Domain Structure Visualization and Other Characterization Techniques for the Application

in the Materials Science and Biomedicine, *Inorganics*, **8**, No. 1: 6 (2020); https://doi.org/10.3390/inorganics8010006
62. A. Schwarz, M. Liebmann, U. Kaiser, R. Wiesendanger, T.W. Noh, and D.W. Kim, Visualization of the Barkhausen Effect by Magnetic Force Microscopy, *Phys. Rev. Lett.*, **92**: 077206 (2004); https://doi.org/10.1103/PhysRevLett.92.077206
63. Y. Kota and A. Sakuma, Mechanism of Uniaxial Magnetocrystalline Anisotropy in Transition Metal Alloys, *J. Phys. Soc. Jpn.*, **83**: 034715 (2014); https://doi.org/10.7566/JPSJ.83.034715
64. L.-Bo. Wu, Y.-F. Fan, F.-B. Sun, K. Yao, and Y.-S. Wang, A Nonlinear Magnetoelastic Energy Model and Its Application in Domain Wall Velocity Prediction, *Sensors*, **22**, No. 14: 5371 (2022); https://doi.org/10.3390/s22145371
65. M. Ohtake, K. Imamura, and M. Futamoto, Magnetostriction, *Handbook of Magnetic Material for Motor Drive Systems*, (Ed. K. Fujisaki) (Springer: 2025); https://doi.org/10.1007/978-981-96-5701-8_15
66. C. Bengtsson, H. Pfutzner, and K. Hoffmann, Domain Modifications Due to Compression Perpendicular to the Rolling Direction of Coated HI-B Sheets, *IEEE Trans. Magn.*, **20**, No. 6: 2116–2119 (1984); https://doi.org/10.1109/TMAG.1984.1063578
67. V.V. Kyrylchuk, Effect of Transition Metal Alloying on Thermal Stability, Structural Relaxation, Crystallization and Magnetic Properties of Amorphous CoSiB Alloys (Abstract of Diss. Cand. Phys.-Math. Sci.) (G.V. Kurdyumov Institute for Metal Physics of the N.A.S. of Ukraine: 2021).
68. I.B. Kekalo and B.A. Samarin, *Physical Metallurgy of Precision Alloys. Alloys with Special Magnetic Properties* (Metallurgiya: 1989), p. 496.
69. J. Díaz, C. Quirós, L. Zárate, L.M. Alvarez-Prado, S. De Panfilis, and J.M. Alameda, Atomic Pair Ordering and Magnetic Anisotropy of Fe–Si Amorphous Films Studied by Linearly Polarized EXAFS, *J. Magn. Magn. Mater.*, **316**, No. 2: e390–e392 (2007); https://doi.org/10.1016/j.jmmm.2007.02.159
70. Y. Nishihara, T. Katayama, Y. Yamaguchi, S. Ogawa, and T. Tsushima, Anisotropic Distribution of Atomic Pairs Induced by the Preferential Resputtering Effect in Amorphous Gd–Fe and Gd–Co Films, *Jpn. J. Appl. Phys.* **17**: 1083 (1978); https://doi.org/10.1143/JJAP.17.1083
71. M.C. Ria, D.W. Ding, B.A. Sun, J.Q. Wang, X.S. Zhu, B.B. Wang, T.L. Wang, Q.Q. Qiu, L.S. Huo, and W.H. Wang, Stress Effects on Magnetic Property of Fe-Based Metallic Glasses, *J. Non-Cryst. Solids*, **495**: 54–58 (2018); https://doi.org/10.1016/j.jnoncrysol.2018.05.017
72. M. Takahashi and T. Kōno, Magnetic Anisotropy Induced by Magnetic and Stress Annealing in Co, Co–Ni and Co–Fe Alloys, *Jpn. J. Appl. Phys.*, **17**: 361 (1978); https://doi.org/10.1143/JJAP.17.361
73. Y. Fu, I. Barsukov, R. Meckenstock, J. Lindner, Y. Zhai, B. Hjörvarsson, and M. Farle, Uniaxial Anisotropy and its Manipulation in Amorphous $Co_{68}Fe_{24}Zr_8$ Thin Films (Invited), *J. Appl. Phys.*, **115**: 172605 (2014); https://doi.org/10.1063/1.4870591
74. N.V. Dmitrieva, V.A. Lukshina, G.V. Kurlyandskaya, and A.P. Potapov, Thermal Stability of Field- and Stress-Induced Anisotropy in Nanocrystalline Fe-Based and Amorphous Co-Based Alloys, *Texture, Stress, and Microstructure*, **32**: 281–287 (1997); https://doi.org/10.1155/TSM.32.281

75. T.J. Egami, Structural Relaxation in Amorphous $Fe_{40}Ni_{40}P_{14}B_6$ Studied by Energy Dispersive X-Ray Diffraction, *J. Mat. Sci.*, **13**: 2587–2599 (1978); https://doi.org/10.1007/BF02402745
76. M. Fabrizio, C. Giorgi, and A. Morro, A Thermodynamic Approach to Ferromagnetism and Phase Transitions, *Int. J. Eng. Sci.*, **47**, No. 9: 821–839 (2009); https://doi.org/10.1016/j.ijengsci.2009.05.010
77. A. Szilva, Y. Kvashnin, E.A. Stepanov, L. Nordström, O. Eriksson, A.I. Lichtenstein, and M.I. Katsnelson, Quantitative Theory of Magnetic Interactions in Solids, *Rev. Mod. Phys.* **95**: 035004 (2023); https://doi.org/10.1103/RevModPhys.95.035004
78. H. Kronmüller, Micromagnetism and Microstructure of Amorphous Alloys (Invited), *J. Appl. Phys.*, **52**, No. 3: 1859–1864 (1981); https://doi.org/10.1063/1.329552
79. Y.S. Kivshar, V.V. Konotop, and Y.A. Sinitsyn, Effect of Fluctuations on the Forced Motion and Interactions of Domain Walls in One-Dimensional Magnetic Systems, *Z. Phys. B – Condens. Matter*, **65**: 209–223 (1986); https://doi.org/10.1007/BF01303845
80. H. Grimm and H. Kronmüller, Investigation of Structural Defects in the Amorphous Ferromagnetic Alloy $Fe_{40}Ni_{40}P_{14}B_6$, *Phys. Status Solidi B*, **117**, No. 2: 663–674 (1983); https://doi.org/10.1002/pssb.2221170228
81. B. Hofmann, T. Reininger, and H. Kronmüller, Influence of the Microstructure on the Magnetization Processes in Nanocrystalline $Fe_{73.5}Cu_1Nb_3Si_{13.5}B_9$, *Phys. Status Solidi A*, **134**, No. 1: 247–261 (1992); https://doi.org/10.1002/pssa.2211340122
82. H. Kronmüller and W. Fernengel, The Role of Internal Stresses in Amorphous Ferromagnetic Alloys, *Phys. Status Solidi A*, **64**, No. 2: 593–602 (1981); https://doi.org/10.1002/pssa.2210640224
83. E.S. Park, Understanding of the Shear Bands in Amorphous Metals, *Appl. Microscopy*, **45**: 63–73 (2015); https://doi.org/10.9729/AM.2015.45.2.63
84. C. Miguel, A.P. Zhukov, and J. Gonzőlez, Stress and/or Field Induced Magnetic Anisotropy in the Amorphous $Fe_{73.5}Cu_1Nb_3Si_{15.5}B_7$ Alloy: Influence on the Coercivity, Saturation Magnetostriction and Magneto-Impedance Response, *Phys. Status Solidi A*, **194**, No. 1: 291–303 (2002); https://doi.org/10.1002/1521-396X(200211)194:1<291::AID-PSSA291>3.0.CO;2-L
85. A.V. Nosenko, V.V. Kyrylchuk, M.P. Semen'ko, M. Nowicki, A. Marusenkov, T.M. Mika, O.M. Semyrga, G.M. Zelinska, and V.K. Nosenko, Soft Magnetic Cobalt Based Amorphous Alloys with Low Saturation Induction, *J. Magn. Magn. Mater.*, **515**, No. 1: 167328 (2020); https://doi.org/10.1016/j.jmmm.2020.167328
86. M. Nowicki, R. Szewczyk, T. Charubin, A. Marusenkov, A. Nosenko, and V. Kyrylchuk, Modeling the Hysteresis Loop of Ultra-High Permeability Amorphous Alloy for Space Applications. *Materials*, **11**, No. 11: 2079 (2018); https://doi.org/10.3390/ma11112079
87. Y. Nykyruy, S. Mudry, Y. Kulyk, V. Prunitsa, and A. Borysiuk, Magnetic Properties and Nanocrystallization Behavior of Co-Based Amorphous Alloy, *Phys. Chem. Solid State.*, **24**, No. 1: 106–113 (2023); https://doi.org/10.15330/pcss.24.1.106-113
88. V.O. Semin, J. Jiang, R.Y. Umetsu, and D.V. Louzguine-Luzgin, Characterization of Fe–Ni–Pt(Zr) Magnetron Deposited Thin Films Subjected to Low-Temperature

Annealing, *Thin Solid Films*, **756**: 139347 (2022);
https://doi.org/10.1016/j.tsf.2022.139347
89. Y. Wu, F. Huang, Z. Chen, H. Liu, J. Zhou, H. Ke, and H. Peng, Structural Aging and Rejuvenation Through Magnetic Annealing in Fe Metallic Glasses, *J. Non-Cryst. Solids*, **6665**: 123608 (2025);
https://doi.org/10.1016/j.jnoncrysol.2025.123608
90. E.N. Tokmakova and V.Yu. Vvedenskiy, Magnetic Properties of the Amorphous Co–Fe–Cr–Si–B Alloy after Annealing in Unsaturated Magnetic Field, *J. Magn. Magn. Mater.*, **594**: 171893 (2024);
https://doi.org/10.1016/j.jmmm.2024.171893
91. I.B. Kekalo and V.Yu. Tsvetkov, Features of the Formation of Magnetic Properties During Annealing and their Temperature-Time Stability in the Amorphous Alloy $Fe_5Co_{58}Ni_{10}Si_{11}B_{16}$, *Phys. Met. Metallogr.*, **59**, No. 3: 490–493 (1985).
92. O. Kohmoto, K. Ohya, N. Yamaguchi, H. Fujishima, and T. Ojima, Amorphous FeCoNi–SiB Alloys Having Zero Magnetostriction, *J. Appl. Phys.*, **51**, No. 8: 4342–4345 (1980);
https://doi.org/10.1063/1.328293
93. T. Miyazaki, T. Oomori, F. Sato, and S. Ishio, Zero Magnetostriction Composition in Fe–Ni–Co Ternary Alloy System, *J. Magn. Magn. Mater.*, **129**, No. 2–3: L135–L136 (1994);
https://doi.org/10.1016/0304-8853(94)90102-3
94. A. Makino, H. Ohmori, and T. Anan, Compositional Effect on Soft Magnetic Properties of Co–Fe–Si–B Amorphous Alloys, *Mater. Trans., JIM*, **31**, No. 10: 884–890 (1990);
https://doi.org/10.2320/matertrans1989.31.884
95. T. Kulik, H. Matyja, and B. Lisowski, Influence of Annealing on Magnetic Properties of Co-Based Metallic Glasses, *J. Magn. Magn. Mater.*, **42**: 135–142 (1984);
https://doi.org/10.1016/0304-8853(84)90091-X
96. J. Jia, Y. Wu, L. Shi, R. Wang, W. Guo, H. Bu, Y. Shao, N. Chen, and K. Yao, Influence of Annealing Process on Soft Magnetic Properties of Fe–B–C–Si–P Amorphous Alloys, *Materials*, **17**, No. 6: 1447 (2024);
https://doi.org/10.3390/ma17061447
97. J. Xu, S. Kang, J. Wang, F Xu, C. Shi, K. Zhang, J. Wang, Z. Chen, J. He, and Z. Sun, Effect of Magnetic Field Annealing on the Soft Magnetic Properties of CoFeSiB Ribbon and its Fluxgate Performance, *J. Magn. Magn. Mater.*, **576**, No. 15: 170762 (2023);
https://doi.org/10.1016/j.jmmm.2023.170762
98. V.R.V. Ramanan, Near-Zero Magnetostrictive Metallic Glasses with very High Saturation Induction, *J. Appl. Phys.*, **53**, No 11: 7822–7824 (1982);
https://doi.org/10.1063/1.330382
99. S. Lu, L. Xu, B. Cao, J. Zhang, H. Duan, and Q. Li, Structural and Magnetic Effects of Mn Addition on CoB Amorphous Alloy by First Principle Simulation, *Results in Physics*, **34**: 105317 (2022);
https://doi.org/10.1016/j.rinp.2022.105317
100. I.B. Kekalo, V.L. Stolyarov, V.Yu. Tsvetkov, Relaxation Processes and Temperature-Time Stability of the Initial Permeability of the Amorphous Alloy $Fe_5Co_{70}Si_{15}B_{10}$, *Phys. Met. Metallogr.*, **55**, No. 6: 1117–1124 (1983).
101. Y. Makino, K. Aso, S. Uedaira, M. Hayakawa, Y. Ochiai, and H. Hotai, Induced Magnetic Anisotropy of Co-Based Amorphous Alloys, *J. Appl. Phys.*, **52**, No. 3: 2477–2479 (1981);
https://doi.org/10.1063/1.328972

102. J. Li, X. Wang, Y. Zhang, H. Liu, and Z. Xu, Influence of Ni Addition on Nanocrystallization Kinetics of Fe–Co-Based Amorphous Alloys, *J. Non-Cryst. Solids*, **434**: 23–27 (2016);
https://doi.org/10.1016/j.jnoncrysol.2015.12.003
103. S. Wang, F. Wang, Y. Liang, H. Jiang, Z. Li, S. Wu, C. Chang, and Z. Cui, Effect of Mn Content on Crystallization Behaviors and Magnetic Properties of FeCoNiBMn High-Entropy Amorphous Alloys, *J. Mater. Res. Technol.*, **28**: 4754–4763 (2024);
https://doi.org/10.1016/j.jmrt.2024.01.052
104. F.L. Kong, C.T. Chang, A. Inoue, E. Shalaan, and F. Al-Marzouki, Fe-Based Amorphous Soft Magnetic Alloys with High Saturation Magnetization and Good Bending Ductility, *J. Alloys Compds.*, **615**: 163–166 (2014);
https://doi.org/10.1016/j.jallcom.2014.06.093
105. X. Qi, J. You, and J. Zhou, A Review of Fe-Based Amorphous and Nanocrystalline Alloys: Preparations, Applications, and Effects of Alloying Elements, *Phys. Status Solidi (A) Appl. Mater. Sci.*, **220**: 2300079 (2023);
https://doi.org/10.1002/pssa.202300079
106. A. Yakin, T. Simsek, B. Avar, T. Simsek, and A.K. Chattopadhyay, A Review of Soft Magnetic Properties of Mechanically Alloyed Amorphous and Nanocrystalline Powders, *Emergent Mater.*, **6**: 453–481 (2023);
https://doi.org/10.1007/s42247-023-00485-0
107. D. Ding, J. You, X. Cui, Y. Xue, X. Tan, and G. Zhai, Application of Amorphous and Nanocrystalline Soft Magnetic Materials in Balanced-Force-Type Electromagnetic Relay, *Micromachines*, **15**: 368 (2024);
https://doi.org/10.3390/mi15030368
108. F.E. Luborsky and J.L. Walter, Magnetically Induced Anisotropy in Amorphous Alloys of Fe–Ni–P–B, *IEEE Trans. Magn.*, **13**, No. 5: 1635–1638 (1977);
https://doi.org/10.1109/TMAG.1977.1059494
109. H.K. Lachowicz, A. Neuweiler, F. Popkawski, and E. Dynowska, On the Origin of Stress-Anneal-Induced Anisotropy in Finemet-Type Nanocrystalline Magnets, *J. Magn. Magn. Mater.*, **173**, No. 3: 287–294 (1997);
https://doi.org/10.1016/S0304-8853(97)00208-4
110. R. Schäfer, Domains in 'Extremely' Soft Magnetic Materials, *J. Magn. Magn. Mater.*, **215–216**: 652–663 (2000);
https://doi.org/10.1016/S0304-8853(00)00252-3
111. V. Zhukova, P. Corte-Leon, L. González-Legarreta, A. Talaat, J.M. Blanco, M. Ipatov, J. Olivera, and A. Zhukov, Review of Domain Wall Dynamics Engineering in Magnetic Microwires, *Nanomaterials*, **10**, No. 12: 2407 (2020);
https://doi.org/10.3390/nano10122407
112. C. Miguel, A. Zhukov, J.J. del Val, and J. González, Coercivity and Induced Magnetic Anisotropy by Stress and/or Field Annealing in Fe- and Co-Based (Finemet-Type) Amorphous Alloys, *J. Magn. Magn. Mater.*, **294**: 245–251 (2005);
https://doi.org/10.1016/j.jmmm.2005.03.041
113. M. Nie, C. Jiang, W. Song, M. Chen, X. Zhao, J. Wang, and H. Guo, Magnetic Domain Structure and Electromagnetic Performance of Amorphous and Nanocrystalline Soft Magnetic Composites Treated by Magnetic Field Assisted Annealing, *J. Alloys Compds.*, **1005**: 175995 (2024);
https://doi.org/10.1016/j.jallcom.2024.175995
114. H. Morita, H. Fujimori, and Y. Obi, Magnetic Anisotropy of Amorphous $(Fe_{1-x}Co_x)_{78}Si_{10}B_{12}$ Alloys, *Appl. Phys.*, **20**: 125–127 (1979);
https://doi.org/10.1007/BF00885932

115. M. Takahashi and S. Ishio, Uniaxial Magnetic Anisotropy in Evaporated Films Caused by the Interaction with Substrate, *Jap. J. Appl. Phys.*, **16**: 579 (1977); https://doi.org/10.1143/JJAP.16.579
116. K. Suzuki, N. Ito, S. Saranu, U. Herr, A. Michels, and J.S. Garitaonandia, Magnetic Domains and Annealing-Induced Magnetic Anisotropy in Nanocrystalline Soft Magnetic Materials, *J. Applied Physics*, **103**: 07E730 (2008); https://doi.org/10.1063/1.2835068
117. I.B. Kekalo and V.A. Klycheva, Features of Structural Relaxation and Formation of Magnetic Properties in High-Cobalt Metalloid-Free Amorphous Alloys with Low Magnetostriction, *Phys. Met. Metallogr.*, **63**, No. 1: 112–119 (1987).
118. I.B. Kekalo, V.Yu. Vvedensky, and V.E. Taranichev, Effect of the Initial Composition of Amorphous Co–Cr–Zr Alloy with Close to Zero Magnetostriction on the Nature of Change in Magnetic Properties During Annealing, *Phys. Met. Metallogr.*, **68**, No. 3: 492–498 (1989).
119. Ł. Madej, G. Haneczok, A. Chrobak, P. Kwapuliński, Z. Stokłosa, and J. Rasek, Long-Term Stability of Soft Magnetic Properties of Amorphous and Nanocrystalline Alloys Based on Iron, *J. Magn. Magn. Mater.*, **320**, No. 20: e774–e777 (2008); https://doi.org/10.1016/j.jmmm.2008.04.105
120. I.B. Kekalo, Effect of Composition and Conditions of Obtaining Amorphous Alloys on the Evolution of Their Magnetic Properties During Annealing (Review) Amorphous (Glassy) Metallic Materials (Science: 1992), p. 107–112.
121. I.B. Kekalo, V.Yu. Tsvetkov, and A.N. Zhdanov, Temporal Instability of the Initial Permeability of the Amorphous Alloy $Fe_5Co_{70}Si_{15}B_{10}$ After Various Types of Magnetic Annealing, *Phys. Met. Metallogr.*, **59**, No. 1: 85–90 (1985).
122. H.-Q. Guo, H. Kronmüller, and N. Moser, Influence of the Induced Anisotropy on the Magnetic After-Effect in Amorphous $Co_{58}Ni_{10}Fe_5Si_{11}B_{16}$ Alloy, *Mater. Sci. Eng.*, **97**: 519–522 (1988); https://doi.org/10.1016/0025-5416(88)90106-1
123. I.B. Kekalo, *Processes of Structure Relaxation and Physical Properties of Amorphous Alloys* (Dom MISiS: 2014), Vol. **2**.
124. P. Allia, C. Beatrice, F. Vinai, A.T. de Rezende, and R. Sato Turtelli, A Study of the After-Effect of the Magnetic Permeability in Co-Rich Amorphous Ferromagnetic Alloys, *J. Appl. Phys.*, **60**, No. 9: 3258–3262 (1986); https://doi.org/10.1063/1.337714
125. Z. Stokłosa, P. Kwapuliński, and M. Karolus, Magnetization Processes in Metallic Glass Based on Iron of FeSiB Type, *Materials*, **15**, No. 24: 9015 (2022); https://doi.org/10.3390/ma15249015
126. H. Kronmüller and M. Wallner, A Review of Magnetic Disaccommodation Effects in Amorphous and Rapidly Solidified Ferromagnetic Alloys, *Phys. Status Solidi A*, **149**: 265–283 (1994); https://doi.org/10.1177/138354169400500105
127. P. Allia, P. Mazzetti, and F. Vinai, Magnetic After-Effects and Structural Instabilities in Amorphous Soft Magnetic Materials, *J. Magn. Magn. Mater.*, **19**: 281–283 (1980); https://doi.org/10.1016/0304-8853(80)90612-5
128. F.E. Luborsky, Kinetics of Reorientation of Magnetically Induced Anisotropy in Amorphous $Fe_{40}Ni_{40}P_{14}B_6$, *AIP Conf. Proc.* **29**: 209–210 (1976); https://doi.org/10.1063/1.30588
129. K. Inomata, M. Hasegawa, and S. Shimanuki, Substituted Amorphous Co–Fe–Si–B Alloys, *Jap. J. Appl. Phys.*, **18**: 937 (1979); https://doi.org/10.1143/JJAP.18.937

130. E. Kisdi-Koszo, P. Vojtanik, and L. Potocky, Magnetic After-Effect in Fe–B Amorphous Alloys, *J. Magn. Magn. Mater.*, **19**: 159–160 (1980); https://doi.org/10.1016/0304-8853(80)90582-X
131. S. Ohnuma, and T. Masumoto, Amorphous Magnetic Alloys (Fe,Co,Ni)–(Si,B) with High Permeability and Its Thermal Stability, *3th Int. Conf. Rapidly Quenched Metals, London: The Metals Socity*, **2**: 197–204 (1978);
132. I.B. Kekalo and P.S. Mogil'nikov, Embrittlement and Conditions of the Optimization of Magnetic Properties in the Amorphous Alloy $Co_{69}Fe_{3.7}Cr_{3.8}Si_{12.5}B_{11}$ in the Absence of a Viscous–Brittle Transition, *Phys. Metals Metallogr.*, **117**: 665–672 (2016); https://doi.org/10.1134/S0031918X16070085
133. J. Luzar, P. Priputen, S. Vrtník, P. Koželj, A. Wencka, D. Gačnik, P. Mihor, B. Ambrožič, G. Dražić, A. Meden, and J. Dolinšek, Zero-Magnetostriction Magnetically Soft High-Entropy Alloys in the $AlCoFeNiCu_x$ ($x = 0.6–3.0$) System for Supersilent Applications, *Adv. Mater. Interfaces*, **9**: 2201535 (2022); https://doi.org/10.1002/admi.202201535
134. A.F. Cobeño, A. Zhukov, A.R. de Arellano-López, F. Elías, J. M. Blanco, V. Larin and J. González, Physical Properties of Nearly Zero Magnetostriction Co-Rich Glass-Coated Amorphous Microwires, *J. Mat. Res.*, **14**, No. 9: 3775–3783 (1999); https://doi.org/10.1557/JMR.1999.0511
135. L. Shi, T. Chai, X. Du, J. Jia, K. Yao, Z. Zhang, and N. Chen, Soft Magnetic Amorphous Alloys and Their Derivatives, *Mat. Sci. Eng., R*, **167**: 101078 (2026); https://doi.org/10.1016/j.mser.2025.101078
136. H.-Q. Guo, B.-G. Shen, D.-M. Lin, and S.-T. Pan, Magnetic Annealing and Crystallization Kinetics of the Metallic Glass $Fe_5Co_{70}Si_{15}B_{10}$, *J. Magn. Magn. Mater.*, **23**: 156–164 (1981); https://doi.org/10.1016/0304-8853(81)90129-3
137. A.I. Taub, Measurement of Microscopic Volume Strain Element in Amorphous Alloys, *Scr. Met.*, **17**, No 7: 873–878 (1983); https://doi.org/10.1016/0036-9748(83)90252-1
138. W. Chambron and A. Chamberod, Structural Relaxation and Atomic Mobility by Magnetic Anisotropy Measurements in Some Metallic Glasses, *J. Phys.*, **42**, No. 5: 511–516 (1981); https://doi.org/10.1051/jphyscol:1981577
139. X.Z. Dong, B. Groger, T. Jendrysik, and H. Kronmüller, Annealing Effect of Domain Patterns of the Nearly Non-Magnetostrictive Amorphous Alloys $Co_{58}Ni_{10}Fe_5Si_{11}B_{16}$, *Phys. stat. sol. (a).*, **71**, No. 2: 441–449 (1982); https://doi.org/10.1002/PSSA.2210710218
140. X.Z. Dong, W. Fernengel, and H. Kronmüller, Annealing Effect and Shortrange Ordering in the Non-Magnetostrictive Amorphous Alloys $Co_{58}Ni_{10}Fe_5Si_{11}B_{16}$, *Appl. Phys. A*, **28**, No. 2: 103–107 (1982); https://doi.org/10.1007/BF00617138
141. S.S.A. Razee, J.B. Staunton, F. Pinski, B. Ginatempo, and E. Bruno, Effect of Atomic Short-Range Order on Magnetic Anisotropy, *Philos. Mag. B*, **78**, Nos. 5–6: 611–615 (1998); https://doi.org/10.1080/13642819808206767
142. I. Mirebeau, V. Pierron-Bohnes, C. Decorse, E. Rivière, C.C. Fu, K. Li, G. Parette, and N. Martin, Magnetic and Atomic Short Range Order in $Fe_{1-x}Cr_x$ Alloys, *Phys. Rev. B*, **100**: 224406 (2019); https://doi.org/10.1103/PhysRevB.100.224406

143. S.K. Kim and O. Tchernyshyov, Mechanics of a Ferromagnetic Domain Wall, *J. Phys.: Condensed Matter.*, **35**, 134002 (2023); https://doi.org/10.1088/1361-648X/acb5d8
144. P.M.E. Icilio Allia, G.P. Soardo, and F. Vinai, Magnetic Permeability After-Effect and Structural Defects of Amorphous Ferromagnetic Alloys, *J. Magn. Magn. Mater.*, **31–34**: 1527–1532 (1983); https://doi.org/10.1016/0304-8853(83)91002-8
145. G. Bottoni, G. Buttino, A. Cecchetti, and M. Poppi, Temperature Dependence of Structural and Magnetic Relaxation in Amorphous and Nanocrystalline Co-Based Alloys, *J. Magn. Magn. Mater.*, **241**: 183–189 (2002); https://doi.org/10.1016/S0304-8853(02)00011-2
146. V.Yu. Vvedenskii and I.B. Kekalo, Theoretical Study of Magneticanisotropy Effects on Initial Permeability of Amorphous Alloys with Near–Zero Magnetostriction, *Phys. Met. Metallogr.*, **81**: 49–56 (1996).
147. V.Y. Vvedenskiy and E.N. Tokmakova, Model of the Hysteresis Loop of Soft-Magnetic Amorphous Alloys with the Usage of a Modified Linear Fractional Function, *Lett. Mater.*, **11**, No. 2: 158–163 (2021); https://doi.org/10.22226/2410-3535-2021-2-158-163
148. J. Chen, L. Yang, and X.-P. Wang, A Reduced Model for Domain Wall Dynamics in Soft Ferromagnets, *J. Magn. Magn. Mater.*, **479**: 199–203 (2019); https://doi.org/10.1016/j.jmmm.2019.02.009
149. P. Braun, F. Jьlicher, and L. Peliti, Domain Wall Motion in Ferromagnetic Layers, *Physica D: Nonlinear Phenomena*, **192**: 249–264 (2004); https://doi.org/10.1016/j.physd.2004.01.022

Received / Final version
02.03.2026 / 02.06.2026

В.В. Кирильчук[1], *В.К. Носенко*[1],
Б.С. Байталюк[1], *І.К. Євлаш*[1], *А.В. Носенко*[1],
В.Є. Яковлев[1], *М.С. Нізамеєв*, *В.А. Дехтяренко*[1,2]
[1] Інститут металофізики ім. Г.В. Курдюмова НАН України,
бульв. Академіка Вернадського, 36, 03142 Київ, Україна
[2] Інститут електрозварювання ім. Є.О. Патона НАН України,
вул. Казимира Малевича, 11, 03150 Київ, Україна

АМОРФНІ СПЛАВИ ЯК ПЕРСПЕКТИВНИЙ КЛАС ФУНКЦІОНАЛЬНИХ МАТЕРІАЛІВ.
Ч. 2. Магнітні властивості, магнітна анізотропія та розбалансування

Робота стосується відомого класу функціональних матеріалів, а саме стрічкових аморфних металевих сплавів на основі Fe та Co. Проаналізовано їхні магнітні властивості, зокрема особливості формування магнітної анізотропії, явища магнітної післядії (розбалансування), а також вплив на них термічних і термомагнітних оброблень. З'ясовано фізичну природу їхньої магнітної м'якості, роль локальних і макроскопічних магнітних анізотропій, магнітопружних ефектів, магнітострикції та доменної структури у формуванні петлі перемагнічування. Зазначено основні джерела їхньої магнітної анізотропії, серед яких визначальну роль відіграє магнітопружна анізотропія, зумовлена внутрішніми напруженнями та магнітострикцією, а також анізотропія спрямованого впорядкування атомних пар. Окрім того, ця магнітна анізотропія є термічно активованим процесом, рушійною силою якого

виступає міжатомна магнітна взаємодія, а ефективність її формування зростає зі зменшенням магнітострикції сплаву. Представлено механізми наведення одновісної анізотропії під час відпалу в магнітному полі та термомеханічного оброблення, а також вплив їх на коерцитивну силу, магнітну проникність і втрати на перемагнічування. Визначено, що температурні та часові нестабільності їхніх магнітних властивостей пов'язані зі стабілізацією меж доменів через спрямоване атомне впорядкування, а дослідження їх виконується за допомогою розбалансування. Показано перспективність використання аморфних магнітом'яких матеріалів із нульовою магнетострикцією в сучасних середньо- та високочастотних електромагнітних пристроях.

Ключові слова: аморфна металева стрічка, магнітні властивості, термічне та термомагнетне оброблення, магнітна анізотропія, розбалансування.